DESIGN AND ANALYSIS OF A BRACELESS STEEL 5-MW SEMI-SUBMERSIBLE WIND TURBINE

Chenyu Luan
Norwegian Research Centre for Offshore Wind Technology, (NOWITECH)
Centre for Ships and Ocean Structures (CeSOS)
Centre for Autonomous Marine Operations and Systems (AMOS), NTNU
NO-7491 Trondheim, Norway
Chenyu.luan@ntnu.no

Zhen Gao
CeSOS and AMOS, NTNU
NO-7491 Trondheim, Norway
Zhen.gao@ntnu.no

Torgeir Moan
CeSOS and AMOS, NTNU
NOWITECH
NO-7491 Trondheim, Norway
Torgeir.moan@ntnu.no

ABSTRACT

This paper introduces the design data and numerical analysis of a braceless steel semi-submersible wind turbine. The hull of the semi-submersible wind turbine is designed to support a reference 5-MW horizontal axis wind turbine at a site in the northern North Sea. The hull is composed of a central column, three side columns and three pontoons. The side columns and pontoons are arranged radially outward from the central column which is used to support the wind turbine. The side columns form the corners of a triangle on the horizontal plane and are connected by the pontoons to the central column at the bottom to form an integrated structure. Numerical analysis has been carried out to analyze the intact stability, natural periods and modes and global dynamic responses in winds and waves. Results of the numerical analysis show that the design has very good intact stability, well designed natural periods and modes, moderate rigid-body motions in extreme environmental conditions and a reasonable structural design. This paper emphasizes the structural responses of the hull considering both the global and local load effects. The global forces and moments in the hull are calculated by carrying out time-domain global analysis and used as inputs for simplified ultimate limit state design checks for structural strength of the hull. The design can be used as a reference semi-submersible wind turbine.

1 INTRODUCTION

Offshore wind energy has become a significant area of development. Offshore wind power has several advantages over onshore wind power [1]. First, offshore wind sites generally produce stronger winds with less turbulence on average because the sea surface is considerably smoother than the land surface. Second, the effects of noise and visual pollution from these sites on humans are negligible because of their distance from populated areas. Third, in most countries, the sea is owned by the government rather than private landlords, which allows for the development of large offshore wind farms. Finally, good sea transport capabilities allow for the construction of large wind turbines with high rated power (e.g., 5-10 MW).

The potential of offshore wind energy is substantial, particularly in relatively deep water (deeper than 80 m). In deep water, floating platforms might be more economically competitive than bottom fixed structures. As compared to spar-type and TLP wind turbines, the advantages of semi-submersible wind turbines include, but are not limited to, 1) greater flexibility in terms of varying sea bed conditions and drafts and 2) significantly reduced installation costs due to their simpler installation, with full assembly at dock[2].

A design challenge is that semi-submersible wind turbines must have sufficient stability and structural strength while the costs of the produced power must be reduced to a competitive level. Natural periods and modes should be well designed to avoid resonant rigid-body motions and structural vibrations excited by loads such as the first order wave loads and 1P and 3P effects.

Semi-submersible wind turbines mainly use side columns to get sufficient intact stability. To reduce the costs of construction and maintenance, most of the proposed semi-submersible wind turbine concepts feature three side columns. The side columns are arranged radially outward from the geometrical center of the water plane area and form the corners of a triangle on the water plane. A wind turbine could be mounted on one side column. Alternatively, the wind turbine

could be mounted on a central column that is located at the geometrical center of the water plane area.

The 5-MW WindFloat is a well-known three-column semi-submersible wind turbine [2,3], while the OC4-Semi is a four-column semi-submersible wind turbine that includes three side columns and a central column [4]. For each design, the columns are connected by braces to form an integrated structure. At a given joint, a column could be connected by several braces. It can be very complex and expensive to weld the joint. Meanwhile, fatigue life of the joint can be a very critical issue due to stress concentration effect at the joint. In addition, to avoid heave resonant motions excited by first order wave loads, additional heave plates and/or pontoons may be needed. Construction of the additional heave plates can be complex and expensive as well.

Braceless semi-submersible wind turbines, for which the columns are connected by pontoons rather than braces, may be a better solution for reducing design complexity and cost of offshore wind power. Several braceless semi-submersible wind turbine concepts, e.g. the 5-MW GustoMSC Tri-Floater [5], VolturnUS [6] and Dr.techn.Olav Olsen's concept[7], have been proposed. However, discussions on structural behaviors of the pontoons in wind- and wave- induced global and local load effects are very limited.

In present paper, we will introduce a design of a braceless steel 5-MW semi-submersible wind turbine. The design is named 5-MW-CSC. The hull of the 5-MW-CSC is designed to support a 5-MW NREL offshore base line wind turbine [8] at a site in the northern North Sea [9].

Numerical analysis has been carried out to analyze the intact stability, natural periods and modes and dynamic global responses in design conditions. The dynamic global responses include rigid-body motions of the hull and global forces and moments in the hull. The global forces and moments in the hull are calculated by carrying out time-domain global analysis and used as inputs for simplified ultimate limit state design checks for structural strength of the hull. Results of the numerical analysis show that the design has very good intact stability, well designed natural periods and modes, moderate rigid-body motions in extreme environmental conditions and a reasonable structural design.

The 5-MW-CSC can be used as a reference semi-submersible wind turbine. A 1:30 model of the 5-MW-CSC has been tested in a hybrid model test by Marintek in October 2015. Rigid-body motions, mooring line tensions and global forces and moments in the tower base and the base of a side column, in winds, waves and currents, are measured. The model test data will be presented, utilized and discussed in other papers in future.

2 DESCRIPTION OF THE DEFINITION OF THE 5-MW-CSC

The definition of the 5-MW-CSC is described in a body-fixed coordinate system (x^b-y^b-z^b). When the 5-MW-CSC is located at its mean positon, the body-fixed coordinate system is coincident to the global coordinate system (x^g-y^g-z^g) shown in Figure 1. The origins of the global and body-fixed coordinate systems (O^g and O^b) are located at the geometrical center of the water plane area. The 0-degree direction of the incident winds and waves is the positive direction of x^g, whereas the 90-degree direction of the incident waves is the positive direction of y^g.

The 5-MW-CSC is composed of a rotor nacelle assembly (RNA), tower, hull and mooring system. The properties of the RNA are described in [8], and the control system and tower are described in [10]. The controller is used to adjust the generator torque and pitch angles of the blades based on the rotational speed of the shaft. The objectives of the controller are 1) optimizing the generated power when the wind turbine is operating in the below rated wind speed and 2) maintain the generated power being at the rated power and avoid the negative aerodynamic damping when the wind turbine is operating in the above rated wind speed. The results presented in the Appendix B show that the rigid-body motions of the 5-MW-CSC in the extreme conditions are very moderate. Details are discussed in the later part of this paper. In addition, both the natural periods in 6 d.o.f.s of rigid-body motions of spar-type and semi-submersible wind turbines are designed similarly in the low frequency range (e.g. above 20 seconds). Consequently, the 5-MW-CSC employs the controller that is described in [10], even though the controller is initially designed for the same wind turbine mounted on a spar-type platform.

The overall dimensions of the hull are given in Table 1. The overall dimensions are a selected result of a parametric study with respect to the effects of the overall dimensions on the intact stability, natural periods, wave induced sectional forces and moments in the hull and cost of the hull. However, the 5-MW-CSC is not developed as an optimized design. It is designed as a 5-MW reference semi-submersible wind turbine with a reasonable structural design of the hull.

The diameter of the central column is set to 6.5 m, which is equal to the diameter of the tower base of the wind turbine. The freeboard of the side columns is 20 m. The distance between the top of the central column and SWL is 10 m. The hull is designed to be constructed by steel with the following properties: density=7,850 [kg/m^3]; Young's modulus= $2.1 * 10^{11}$[Pa]; yield stress=235 [MPa]; Poisson's ratio=0.3; and structural damping ratio=1%.

The ratio of the total steel weight to the displacement is approximately 0.17, yielding the equivalent thickness of the hull to be 0.03 m. The global and local load effects at the lower part of the columns, pontoons and joints are more critical than the load effects at the upper part of the columns. The thickness of each component can be adjusted based on a more detailed analysis to improve fatigue life and ultimate strength. Adjustments to the thickness have a negligible effect on the stability, rigid-body motions and global forces and moments in the hull because the displacement is considerably larger than the steel weight.

A ballast distribution for the operating draft is shown in Figure 3. The ballast mass are symmetrically distributed about the central line of the central column. Ballast water is used to

achieve the operating draft, and the pontoons are completely filled with ballast water. The pressure head of the ballast water in each side column is 7.7 m as measured from the top of the pontoon. Meanwhile, no ballast water is used in the central column. Mass and moment of inertia of the hull are given in Table 2. The mass properties are calculated by assuming that the ballast water inside the columns and pontoons does not contribute any free surface.

The mooring system is composed of three catenary chain mooring lines. The chain mooring lines are simplified as a uniformly distributed mass with a solid circle cross-section. The design parameters are given in Table 3. The axial stiffness is $3.08 * 10^6$ kN/m. The bending stiffness and torsional stiffness are set to zero.

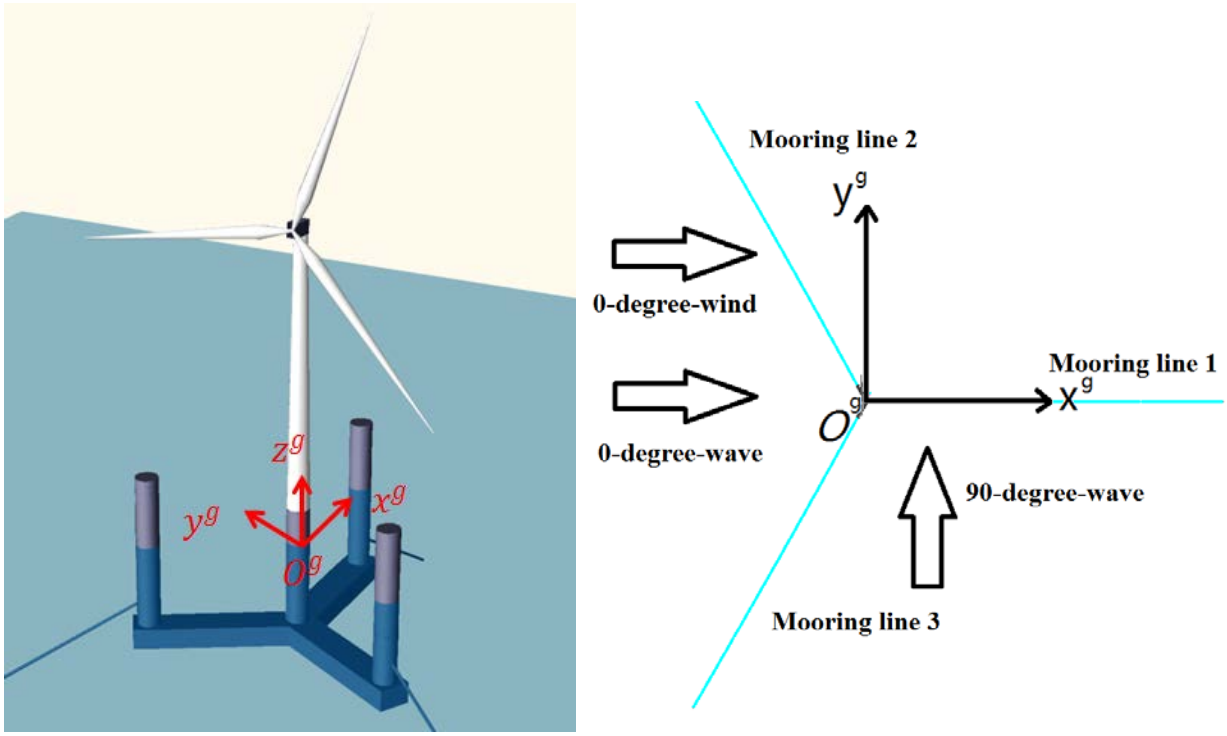

Figure 1 Layout of the 5-MW-CSC

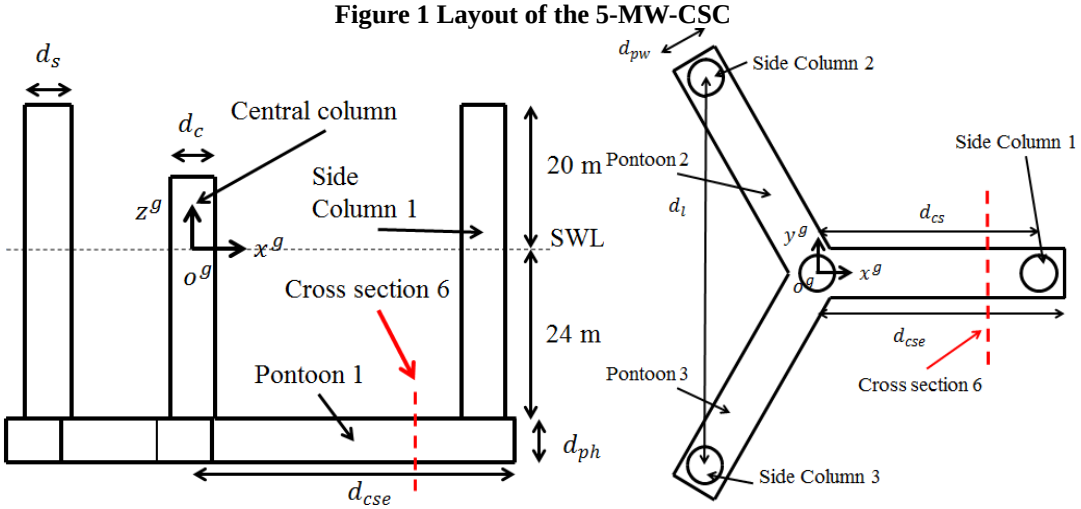

Figure 2 Side (left) and top (right) views of the hull of 5-MW-CSC

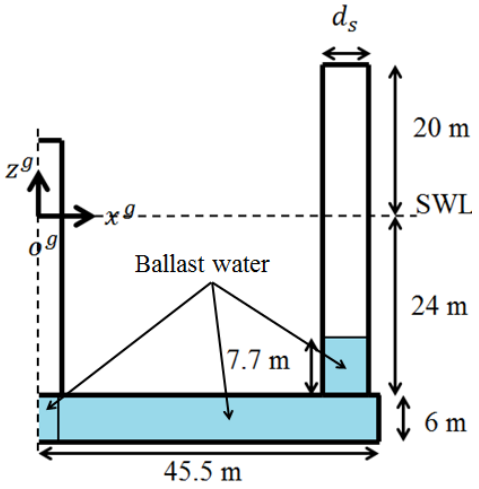

Figure 3 Ballast distribution

Table 1. Dimensions of the hull of the 5-MW-CSC

d_c [m]	6.5
d_s [m]	6.5
d_{ph} [m]	6
d_{pw} [m]	9
d_{cs} [m]	41
d_{cse} [m]	45.5
Operating draft [m]	30
Displacement [tonne]	10,555
Steel weight [tonne] (hull)	1,804
Equivalent thickness [m]	0.03

Table 2 Mass properties of the hull of the 5-MW-CSC (including steel and ballast water). The center of gravity and moments of inertia are described in the body-fixed coordinate system with respect to O^b

Mass [tonnes]	Center of gravity [m]			Moments of inertia [tonnes*m^2]					
	x^b	y^b	z^b	I_{xx}	I_{yy}	I_{zz}	I_{xy}	I_{xz}	I_{yz}
9,738	0	0	-24.36	$1.05 * 10^7$	$1.05 * 10^7$	$8.24 * 10^6$	0	0	0

Table 3. Design parameters of a single mooring line

Mass per unit length (in the air) [tonne/m]	0.115
Pretension at the fairlead [kN]	1,683
Un-stretched mooring line length [m]	1,073
Diameter of the mooring line cross-section [m]	0.137
Density of the material [tonne/m^3]	7.85
Clump weight in water[tonne]	15
Distance from the attachment point of the clump weight to the fairlead (along the mooring line) [m]	240

Table 4. Arrangement of the mooring line anchors and fairleads described in the global coordinate system

Fairlead	x^g	y^g	z^g
1	44.3	0	-18
2	-22.1	38.3	-18
3	-22.1	-38.3	-18
Anchor	x^g	y^g	z^g
1	1,084.4	0	-200
2	-542.2	939.1	-200
3	-542.2	-939.1	-200

Table 5. Selected design conditions (from the contour surface corresponding to a 50-year return period)

Environmental condition	Mean wind speed at nacelle height	Turbulence intensity [%]	H_s [m]	T_p [s]	Note
	[m/s]				
Selected design conditions for analysis of motion responses in extreme conditions					
EC1	9.8	16	7.5	14.7	In operation
EC2	11.4	15	7.9	14.4	
EC3	16	13	9.14	15.0	
EC4	20	12	10.3	14.7	
EC5	40.4	11	15.3	14.3	Parked
Selected design conditions for the simplified ULS design check for structural strength of the hull					
U0101	4.9	23	4.6	8	In operation
U0102	4.9	23	6.1	18	
U0103	4.9	23	4.7	24	
U0201	8.0	17	5.2	8	
U0202	8.0	17	6.7	18	
U0203	8.0	17	5.3	23	
U0301	11.0	15	5.7	8	
U0302	11.0	15	7.3	18	
U0303	11.0	15	5.5	23	
U0401	16.5	13	6.5	8	
U0402	16.5	13	8.4	18	
U0501	21.3	12	7.1	8	
U0502	21.3	12	10.4	16	
U0601	25.4	11.7	7.5	8	Parked
U0602	25.4	11.7	11.9	15	
U0701	30.0	11.2	8.7	9	
U0702	30.0	11.2	13.3	15	
U0801	34.6	11.1	8.7	9	
U0802	34.6	11.1	14.6	15	

U0901	39.8	11.1	10.5	11	
U0902	39.8	11.1	15.3	14	

3 DESIGN CONDITIONS

Joint probability density function of mean wind speed, significant wave height (H_s) and peak period of wave spectrum (T_p) and a 3-D contour surface of the mean wind speed, H_s and T_p corresponding to the 50-year return period are described in [9]. Two-parameter JONSWAP spectrum is employed to describe the waves, while the winds are described by Kaimal wind spectrum with normal turbulence. Wind class is assumed as class C (low turbulent wind). The turbulent intensity factors are given in [11].

To address motions of the 5-MW-CSC in extreme combined wind and wave conditions, five mean wind speeds (from EC1 to EC5), including a wind speed below the rated speed, a wind speed at the rated speed, two wind speed above the rated speed and an extreme wind speed, are selected and tabulated in Table 5. The mean wind speeds in the table are referred to the position of the nacelle.

The points, which are located on the 3-D contour surface and correspond to a given mean wind speed, can form a closed circle in a 2-D plane with respect to H_s and T_p.

For each mean wind speed, the largest H_s on the corresponding closed circle and the T_p, which corresponds to the largest H_s, are selected. In EC 5, the selected H_s is 0.1 m smaller than the largest H_s of all the points on the 3-D contour surface.

In addition, a simplified ULS design check for the hull is carried out based on 21 design conditions (from U0101 to U0902) selected from the 3-D contour surface that corresponding to the 50-year return period. The design conditions are tabulated in Table 5

4 CASE STUDY FOR THE 5-MW-CSC

4.1 INTACT STABILITY ANALYSIS

The intact stability is checked based on the righting and overturning moment curves. The overturning moments come from aerodynamic loads on the RNA, tower and hull and make the semi-submersible wind turbine rotate with respect to an axis in the water plane area. The geometrical center of the water plane area is always on the axis. For example, the overturning moments induced by constant winds along x^g result in heeling angles with respect to a rotation axis that is in parallel to y^g. Righting moment is generated by hydrostatic pressure forces on the wet surface of the hull and gravity of the semi-submersible wind turbine. To find the most critical situation, righting moment curves corresponding to several different rotational axes need to be calculated and checked. In this paper, we make the rotational axis constantly be in parallel to y^g while the semi-submersible wind turbine is rotated by ϕ degrees with respect to z^g. Since the semi-submersible wind turbine is symmetrical with respect to the $x^g - z^g$ plane, ϕ varies from 0 degrees to 180 degrees with 15-degree intervals. For each righting moment curve, heeling angle varies from 0 degrees to 90 degrees.

Aerodynamic loads on the hull and tower are calculated by Riflex [12]. To simplify the calculation and to be conservative, we neglect the shielding, solidification and finite length effects described in [13] and assume that incident winds are constantly and uniformly distributed from the sea level up to the tower top. The aerodynamic loads on a given cross-section of the tower or a given cross-section of a given column can be expressed by the drag term of the Morison formula [13]. The non-dimensional drag coefficient for the cross-section of the tower or the column is specified as 0.65. Wind loads on the pontoons are not considered even through, under a very large heeling angle, part of the pontoons may be raised from water to air. The aerodynamic loads on the rotor are calculated in Aerodyn [14].

Wind induced forces are in line to the direction of the incident winds. Consequently, for a given ϕ, the maximum overturning moment with respect to the rotational axis is given by the 0-degree-winds, which is project to the rotational axis. Therefore, for each ϕ, overturning moments induced by the 0-degree-winds are calculated. We assume that the rotor plane is always projected to the 0-degree-wind and the restoring forces are always acting on the geometrical center of the three fairleads of the mooring lines.

The overturning moments induced by wind loads on the tower and central column are independent to ϕ and proportional to square of cosine of the heeling angle. Due to distribution of the side columns, when the heeling angle is in the range of 0 degrees to 30 degrees, overturning moments induced by wind loads on the side columns are insensitive to ϕ. An example is shown in Figure 4.

Overturning moments induced by wind loads on the rotor in operational and parked conditions and by wind loads on the tower and hull at 0-degree-heeling angle are shown in Figure 5. Aerodynamic loads on the rotor contribute most of the overturning moments in the operational condition. In the parked condition, the overturning moments are proportional to square of mean wind speed and can be critical in extreme winds, e.g. 50 m/s extreme wind at nacelle.

The criterion specified in the DNV-OS-J103 [15] is utilized to check the intact stability of the 5-MW-CSC. We assume that the ballast mass will not introduce a free surface inside the hull. To simplify the calculation and to be conservative, design overturning moment (DOM) is specified as a constant value with respect to the heeling angle. The DOM is independent to Φ and the heeling angle. The constant value is specified as 90,000 kN*m which is obtained by applying a 1.2 safety factor on the most critical overturning moment. The most critical overturning moment is 75,000 kN*m given by the operational condition with 11 m/s mean wind speed. We assume that the hull is an integrated watertight structure without openings on the hull and water will entry to the tower if the central column is submerged in water. Figure 6 shows that the most critical

situation for the intact stability analysis is given by $\phi = 0$. In general, a given righting moment curve and a design overturning moment curve will have two intersections. The ratio of the area under the righting moment curve ($\phi = 0$) from 0 degrees to the second intersection to the corresponding area under the DOM is 1.63, which is larger than 1.3 and satisfies the intact stability criterion. In addition, the DOM inherently includes a large safety margin as well.

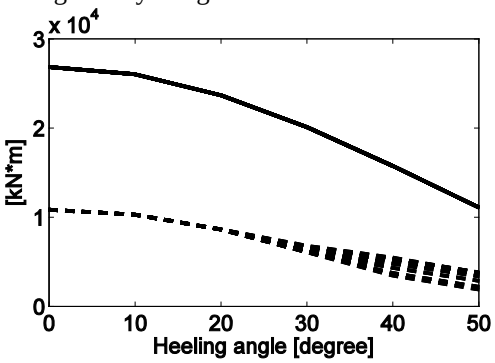

Figure 4. Overturning moment curves induced by 50 m/s constant wind loads on the tower and central column (the solid lines) and on the side columns (the dash lines). ϕ varies from 0 degrees to 180 degrees with 10-degree intervals. Heeling angle varies from 0 degrees to 50 degrees with 10-degree intervals.

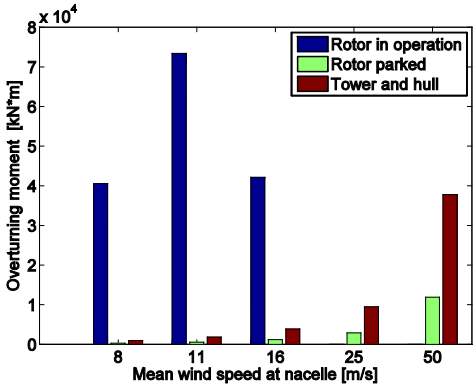

Figure 5 Overturning moments induced by wind loads on the rotor in operational and parked conditions and by wind loads on the tower and hull at 0-degree-heeling angle

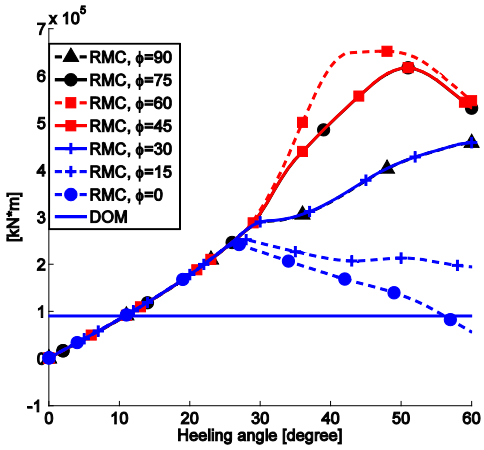

Figure 6 Righting moment curve (RMC) v.s. design overturning moment curve (DOM), intact stability analysis

4.2 NATURAL PERIODS AND MODES

The natural periods of the 6 degrees of freedom rigid-body motions of the 5-MW-CSC are calculated by numerical decay tests and tabulated in Table 6. The numerical model used in the decay tests is denoted as TMD2 and described in the paper [16]. The hull is assumed as a single rigid-body with 6 d.o.f.s. Slender structures, such as blades, shaft of drive train, tower and catenary mooring lines, are modelled by beam elements.

A pure beam model of the 5-MW-CSC (the mooring lines, hull, tower and RNA are modelled by corresponding equivalent beam elements) is developed in Riflex [12] to calculate the other natural periods and modes (structural vibrations). The ballast water inside the pontoons does not contribute to global stiffness. The mass of the beam elements accurately accounts for the mass distribution of the hull (including steel mass and ballast mass). Stiffness of the beam elements for the central column and side columns are calculated based on a circle cross-section with 6.5 m diameter and 0.03 m thickness, while stiffness of the beam elements for the pontoons are calculated based on a box-shape cross-section with 6 m height, 9 m width and 0.03 m thickness. Mooring lines' flexibility is accounted for by using bar elements.

The natural periods and modes are calculated based on Lanczos' method. Effects of added mass, gravity, hydrostatic pressure forces on the natural modes are accounted for by the Riflex. The results indicate that the natural periods of the natural modes, which are related to the pontoons and columns, are in the range of 1.6 to 3 seconds, which is beyond the range of the main wave energy. For the 5-MW NREL reference wind turbine, 1P is in the range of 5 to 8.7 seconds, while the 3P is in the range of 1.7 to 2.9 seconds. However, due to the shape of the natural modes of the pontoons and columns, such as the hogging and sagging modes of the hull, the vibrations of the pontoons and columns due to the 3p effect are negligible.

Table 6. Natural periods ([s]) of the 6 degrees of freedom rigid-body motions of the 5-MW-CSC

Surge	Sway	Heave	Roll	Pitch	Yaw
79.5	79.5	25.8	31.28	31.32	58.12

4.3 RIGID-BODY MOTIONS

The transfer functions for wave induced rigid-body motions are calculated by WADAM [17]. The transfer functions are related to the wave direction and shape of the hull. Some representative transfer functions are presented in Appendix A. We focus on the transfer functions in the range of 0.314 rad/s to 2 rad/s. The peaks and troughs in the frequency range indicate that the radiation effect and wave diffraction effect are important. Viscous loads on the hull and restoring stiffness of the catenary mooring lines have very limited effects on the transfer functions in the wave frequency range and are not accounted for.

The 5-MW-CSC exhibits relatively small motions under different combined wind and wave conditions, even in extreme wind and wave conditions. This is because 1) the pontoons of the 5-MW-CSC provide relatively large viscous damping and potential damping, 2) water plane area is relatively small, 3) the draft of the 5-MW-CSC is relatively large, and 4) the natural periods are well designed to be away from the wave frequency range.

Time-domain simulations based on the five environmental conditions (from EC1 to EC5) described in the Table 5 are carried out to check the rigid-body motions of the 5-MW-CSC in extreme combined wind and wave conditions. The numerical model employed by these time-domain simulations is identical to the TDM2 [16] except that mean drift forces and slow varying drift forces on the hull are included through the Newman's approximation. In the time-domain simulations, the direction of the incident winds is constantly specified as 0 degrees, while, 19 different wave directions are specified (from 0 to 180 degrees with 10 degrees interval).

Statistical properties of the rigid-body motions, i.e. mean, standard deviation, maximum and minimum, are calculated based on stationary time series. To account for statistical uncertainty, in this section, we only discuss the averaged statistical properties. For a given environmental condition with a given wave direction, the averaged statistical properties are calculated based on ten 1-h time-domain simulations with different random seeds. The averaged statistical results are given in Appendix B. The main observations are illustrated as follows.

The 5-MW-CSC has very limited heave motions in most of the operational conditions, where H_s could be less than 4 m. For example, in the EC1, where H_s is 7.5 m and T_p is 14.7 seconds, maximum 1-h heave motion is less than 2.4 m and the standard deviation is 0.7 m. The most critical heave motion is given by the EC5, in which the 1-h heave motion is in range of -5 m to 5.5 m and standard deviation is 1.5 m. The heave motion is independent to directions of winds and waves.

The 1-h pitch motion is in range of -3 degrees to 10 degrees. When the rotor is in operation, the pitch motion is dominated by wind loads. When the rotor is parked, wave loads dominate the pitch motion. The 1-h pitch motion standard deviation is in range of 0.3 degrees to 1.8 degrees. Compared to the statistical properties of the WindFloat given by [18], the 5-MW-CSC has more moderate pitch motions in combined winds and waves. The 1-h roll motion is in range of -4 degrees to 3.2 degrees. The roll motion is dominated by wave loads except that, when the rotor is in operation, the aerodynamic torque on the rotor results in a mean roll motion.

Regarding horizontal motions, 1-h surge, sway and yaw motions are in range of -7 m to 11 m, -5 m to 9 m and -2.25 degrees to 2.5 degrees respectively. Surge and sway motions are referred to the center of the water plane area rather than the center of gravity of the 5-MW-CSC. The moderate horizontal motions could be good for power cable design.

No instable motions, which might be induced by the misalignment of the winds and waves, are observed.

4.4 SIMPLIFIED ULS DESIGN CHECK BASED ON A LIMITED NUMBER OF DESIGN CONDITIONS

The pontoons of the 5-MW-CSC are composed of stiffened plates, girders and bulkheads. We focus on buckling strength design check for the stiffened plates of the pontoons.

A stiffened plate is shown in Figure 7. We assume that the stiffened plate is located at bottom of the Pontoon 1 and is nearby a specified cross-section of the Pontoon 1. The specified cross-section is shown by the red dashed line in Figure 2. In addition, the stiffened plate is assumed to be located in between of two transverse girders and the side surfaces of the pontoon. Therefore, the width of the stiffened plate (l_2) is equal to the width of the Pontoon 1 which is 9 m. We assume that the distance between the girders is 3m. Consequently, the length of the plate (l_1) is 3 m.

We assume that the thickness of the plate is 0.016 m, the span (s) for the T stiffeners on the plate is 0.5 m, the web height and flange length of the T stiffeners is 0.5 m and 0.2 m. The web thickness and flange thickness is 0.008 m and 0.016 m. Consequently, the steel weight of the stiffened plate is equal to the steel weight of a plate with the same length and width and 0.0315 m thickness, which is very close to the equivalent thickness of the hull. However, the steel weight of the girders is not included yet. To estimate the steel weight of the girders, at least, a preliminary design for structural details of the pontoons need to be developed in future. The estimated steel weight of the hull can be maintained since the global and local load effects on the upper part of the columns are less critical than the global and local load effects on the lower part of the columns, pontoons and joints. Adjustments to the thickness have a negligible effect on the stability, rigid-body motions and global forces and moments in the hull because the displacement is considerably larger than the steel weight.

The stiffened plate is subjected to σ_{hp}, σ_1, σ_2 and τ_{12}. σ_{hp} represents hydro-pressure on the plate. The hydro-pressure includes hydrostatic pressure and hydrodynamic pressure on the outer surface of the plate and the ballast water induced pressure on the inner surface of the plate. σ_1 represents nominal uniform stress in stiffener direction. σ_2 represents nominal

uniform stress in perpendicular to stiffener direction. τ_{12} represents shear stress. σ_1 and τ_{12} can be derived from the global forces and moments in the specified cross-section of the Pontoon 1.

Global time-domain analysis is carried out to calculate the global forces and moments in the combined wind and wave conditions described in Table 5. The hull of the 5-MW-CSC is a static determinate structure, while, the specified cross-section divides the hull into two parts (Part A and Part B). The wind turbine is mounted on the Part B. The global forces and moments in the specified cross-section can be determined under the condition of the force and moment equilibrium considering the inertia loads of the Part A and the corresponding hydro-loads on the Part A. The inertia loads are induced by the global rigid-body motion of the hull in combined winds and waves. Potential-flow theory can be employed to account for the first order added mass, potential damping and wave excitation loads on the Part A.

We use TDM3, which is a time-domain numerical model developed by Luan et al [16], to calculate the global forces and moments in a straight-forward manner. Luan et al [16] verified that the TDM3 can accurately calculate the global forces and moments in the hull on the conditions that 1) the hull is a static determinate structure, 2) the hull is very stiff, and 3) second and higher order hydrodynamic loads on the hull are not significant.

We assume that the global behavior of the pontoons of the hull can be accounted for by the Euler-Bernoulli beam theory. The cross-section can be simplified as a thin-wall box-shape cross-section shown in Figure 8. Eight points are specified on the cross-section. F_x, F_y, F_z, M_x, M_y, and M_z denote the global forces and moments in the cross-section in the x_{inp}-y_{inp}-z_{inp} coordinate system. The x_{inp}-y_{inp}-z_{inp} coordinate system is a body-fixed coordinate system. The x_{inp}-y_{inp}-z_{inp} coordinate system is coincident to the body-fixed coordinate system of the 5-MW-CSC (x^b-y^b-z^b) except that the origin of the x_{inp}-y_{inp}-z_{inp} coordinate system is located at (31.5, 0, -27) in the x^b-y^b-z^b coordinate system.

For a given point on the cross-section, normal stress (σ_x) and shear stress (τ) are calculated by Eqs.(1,2).

$$\sigma_x = \frac{F_x}{A} + \frac{M_y}{w_{y_{inp}}} + \frac{M_z}{w_{z_{inp}}} \qquad (1)$$

$$\tau = \frac{M_x}{2A_0 t_c} + \frac{F_y S_{z_{inp}}}{I_{z_{inp}} t_c} + \frac{F_z S_{y_{inp}}}{I_{y_{inp}} t_c} \qquad (2)$$

A is the area of the cross-section. $w_{y_{inp}}$ and $w_{z_{inp}}$ are the section moduli corresponding to the y_{inp} and z_{inp} axes and the position of the point on the cross-section. A_0 is the circumscribed area of the cross-section. $S_{y_{inp}}$ and $S_{z_{inp}}$ are static moments corresponding to the y_{inp} and z_{inp} axes and the position of the point on the cross-section. $I_{y_{inp}}$ and $I_{z_{inp}}$ are the second moments of area of the cross-section.

To calculate A, $w_{y_{inp}}$ and $w_{z_{inp}}$, the thickness of the thin-wall of the box-shape cross-section is specified as 0.03 m, which is slightly smaller than the equivalent thickness estimated based on the steel weight of the stiffened plate (0.0315 m) and on the safe side.

In the global analysis, torsional stiffness and shear stiffness of the cross-section are mainly provided by the plates of the pontoon. Contribution of the T stiffeners on the plates to the torsional stiffness and shear stiffness is negligible. Therefore, to calculate the $S_{z_{inp}}$, $S_{y_{inp}}$, A_0, $I_{z_{inp}}$ and $I_{y_{inp}}$ in Eq.(8), the thickness of the thin-wall of the box-shape cross-section is specified as 0.016 m which is equal to the thickness of the plates of the pontoon. Consequently, t_c, in Eq.(8), is 0.016 m.

For each design condition, 10 1-h time-domain simulations are conducted to account for statistical uncertainty. For each 1-h time-domain simulation, simulation length is 4,600 seconds. The first 1,000 seconds is considered as transient process and is excluded in post-analysis. We find that averaged ranges of the normal stress (σ_x) and shear stress (τ) of the eight points on the cross-section in the 21 design conditions are -83 MPa to 38 MPa and -21 MPa to 28 MPa respectively.

Buckling utilization factors for the stiffened plate in all the combinations of the design loads, i.e. σ_{hp}, σ_1, σ_2 and τ_{12}, are calculated by using the S3 element code of PULS [19]. PULS is a computerized buckling code for thin-walled plate construction and accepted by DNV-RP-C201 [20] for checking buckling strength of plated structures. The code implements the Marguerre's non-linear plate theory in combination with stress control criteria. The boundary conditions for the edges of the stiffened plate are described in [19].To be conservative, we specify the hydro-pressure on the stiffened plate (σ_{hp}) as 0.5 MPa although the operating draft is 30 m. The ranges of the nominal uniform stress in stiffener direction (σ_1) and shear stress (τ_{12}) are obtained by applying a 1.3 load factor on the averaged ranges of the normal stress (σ_x) and shear stress (τ) respectively. Consequently, we specify that the σ_1 varies in the range of -110 MPa to 50 MPa with 10-MPa intervals, while τ_{12} varies in the range of -30 MPa to 40 MPa with 10-MPa intervals. The combinations of the σ_1 and τ_{12} are on the safe side since the critical value of σ_1 and critical value of τ_{12} may not necessarily appear at the same time and/or at the same position on the cross-section. We assume that the nominal uniform stress in perpendicular to stiffener direction (σ_2) is induced by hydrostatic pressure forces on the side surfaces of the pontoon. We specify σ_2 as -60 MPa.

The maximum buckling utilization factor is 0.62 and indicates that the stiffened plate has sufficient buckling strength. The buckling utilization factors are very sensitive to the length of the stiffened plate (l_1). The maximum buckling utilization factor will be increased from 0.62 to 1.14 if the l_1 is increased from 3 m to 4 m.

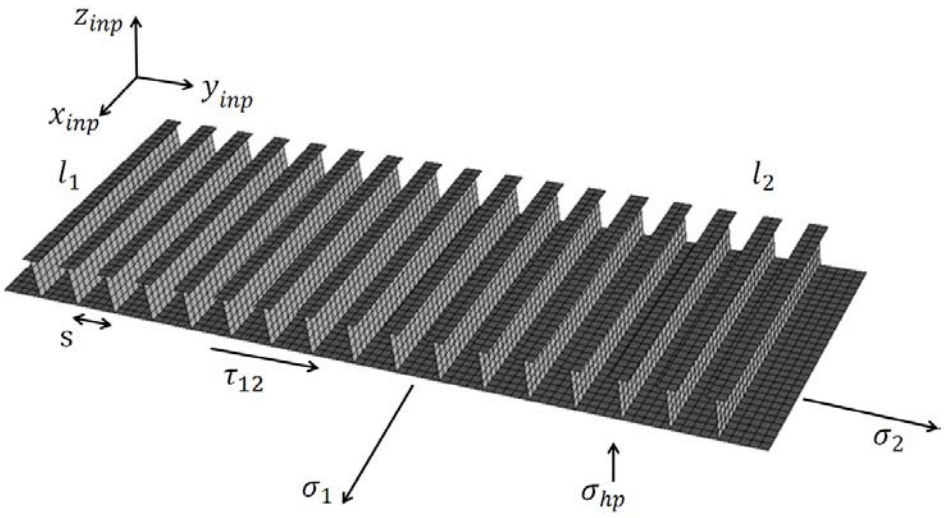

Figure 7 stiffened plate of the bottom of the Pontoon 1 of the 5-MW-CSC

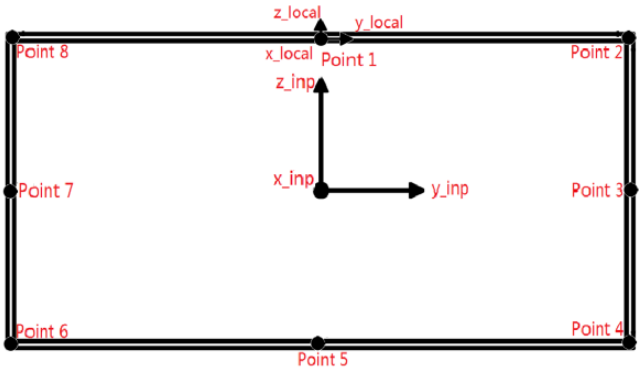

Figure 8 A simplified thin-wall box-shape cross-section (for global analysis)

5 CONCLUSIONS

Design of a braceless steel semi-submersible wind turbine has been introduced in present paper. The hull of the design is composed of a central column, three side columns and three pontoons and designed to support the 5-MW NREL reference wind turbine in offshore sites with harsh environmental conditions, e.g. the northern North Sea. Dimensions of the columns and pontoons, distributions of ballast water and steel and design parameters of the mooring system have been tabulated.

The design has very good intact stability. The intact stability of the design has been checked based on the righting and overturning moment curves. In the most critical situation, the ratio of the area under the corresponding righting moment curve from 0 degrees to the second intersection to the corresponding area under the design overturning moment curve is 1.63, which satisfies the intact stability criterion.

Natural periods and modes of the design have been well designed to avoid resonant rigid-body motions and structural vibrations excited by the 1P effect and first order wave loads. Due to the shape of the natural modes of the pontoons and columns, the 3P effect excited vibrations of the pontoons and columns are negligible.

The design exhibits relatively small motions under different combined wind and wave conditions. In extreme wind and wave conditions, 1-h surge, heave, pitch and yaw motions are in range of -7 m to 11 m, -5 m to 5.5 m, -3 degrees to 10 degrees and -2.25 degrees to 2.5 degrees respectively. No instable motions, which are induced by the misalignment of the winds and waves, are observed.

PULS has been used to check ultimate strength of a stiffened plate at the bottom of the Pontoon 1. We assume that the stiffened plate is nearby a specified cross-section of the Pontoon 1. Specifications for the sizes and thickness of the plate and spans and dimensions of the T stiffeners have been given. The steel weight of the stiffened plate is close to the corresponding estimated steel weight.

PULS accounts for local and global load effects on the ultimate strength of the stiffened plate. Buckling utilization factors for the stiffened plate in all the combinations of the design loads, i.e. σ_{hp}, σ_1, σ_2 and τ_{12}, have been calculated by using the S3 element code of PULS.

The nominal uniform stress in stiffener direction (σ_1) and shear stress (τ_{12}) have been derived from the global forces and moments in the specified cross-section of the Pontoon 1. Global time-domain analysis has been carried out to calculate the global forces and moments in 21 selected combined wind and wave design conditions.

The maximum buckling utilization factor is 0.62 and indicates that the stiffened plate has sufficient buckling strength. The buckling utilization factors are very sensitive to the distance of the girders of the pontoon.

ACKNOWLEDGMENTS

The authors acknowledge the financial support provided by the Research Council of Norway granted through the Centre for Ships and Ocean Structures; the Norwegian Research Centre for Offshore Wind Technology (NOWITECH), NTNU; and the Centre for Autonomous Marine Operations and Systems (AMOS), NTNU. Partial financial support from the EU FP-7 project MARINA Platform project (Grant Agreement 241402) is also acknowledged.

REFERENCES

[1] Twidell, J. and Gaudiosi, G., (2009), "*Offshore Wind Power*", Multi-Science Publishing Co.Ltd.

[2] Roddier, D., Cermelli, C., Aubault, A., and Weinstein, A., (2010), "WindFloat: A floating foundation for offshore wind turbines", Journal of Renewable and Sustainable Energy 2, 033104, doi:10.1063/1.3435339.

[3] Roddier, D., Peiffer, A., Aubault, A., and Weinstein, J., (2011), "A generic 5 MW WindFloat for numerical tool validation & comparison against a generic spar", In 30th International Conference on Ocean, Offshore and Arctic Engineering, no, OMAE2011-50278, Rotterdam, the Netherlands.

[4] Robertson, A., Jonkman, J., Masciola, M., Song, H., Goupee, A., Coulling, A., and Luan C., (2012), "Definition of the Semisubmersible Floating System for Phase II of OC4", Offshore Code Comparison Collaboration Continuation (OC4) for IEA Task 30.

[5] Huijs, F., Mikx, J., Savenije, F., and Ridder, E., (2013), "Integrated design of floater, mooring and control system for a semisubmersible floating wind turbine", European Wind Energy Association (EWEA) Offshore, Frankfurt.

[6] Viselli, A. M., Goupee, A. J., and Dagher, H., (2014), "Model Test of a 1:8 Scale Floating Wind Turbine Offshore in the Gulf of Maine", In 33th International Conference on Ocean, Offshore and Arctic Engineering, no, OMAE2014-23639, San Francisco, CA, USA.

[7] Dr.techn.Olav Olsen AS, (2015), http://www.olavolsen.no/en/node/17, accessed 8.April.2015.

[8] Jonkman J., Butterfield, S., Musial, W. and Scott, G., (2009), "Definition of a 5-MW Reference Wind Turbine for Offshore System Development", NREL/TP-500-38060, National Renewable Energy Laboratory, Golden, CO, U.S.A.

[9] Li, L., Gao, Z., Moan, T., (2015), "Joint Distribution of Environmental Condition at Five European Offshore Sites for Design of Combined Wind and Wave Energy Devices", Journal of Offshore Mechanics and Arctic Engineering. 137(3), 031901 (16 pages). doi: 10.1115/1.4029842.

[10] Jonkman J., (2010), "Definition of the Floating System for Phase IV of OC3", NREL/TP-500-47535, National Renewable Energy Laboratory, Golden, CO, USA

[11] IEC, (2005), "Wind turbines – Part 1: Design requirements", IEC-61400-1, International Electrotechnical Commission.

[12] MARINTEK, (2013). RIFLEX User's Manual.

[13] DNV, (2010), "Recommended Practice - Enivronmental Conditions and Environmental Loads", DNV-RP-C205, Det Norske Veritas.

[14] Moriarty, P. J., and Hansen, A. C., (2005), AeroDyn theory manual, Tech. Rep, NREL/TP-500-36881.

[15] DNV, (2013), "Offshore standard – Design of Floating Wind turbine Structures", DNV-OS-J103, Det Norske Veritas.

[16] Luan, C., Gao, Z. and Moan, T., (2016), "Development and verification of a comprehensive time-domain approach for determining forces and moments in structural components of floating wind turbines", Plan to be submitted to Marine structures.

[17] DNV, (2013), SESAM User Manual HydroD.

[18] Gao, Z., Luan, C., Moan, T., Skaare, B., Solberg, T. and Lygren, J.E., (2011), "Comparative Study of Wind- and Wave-Induced Dynamic Responses of Three Floating Wind Turbines Supported by Spar, Semi-Submersible and Tension-Leg Floaters". Proceedings of the 2011 International Conference on Wind Energy and Ocean Energy (ICOWEOE'11). 31 October- 2 November 2011 - Beijing, China.

[19] DNV, (2009), "Nauticus Hull User Manual PULS", Det Norske Veritas.

[20] DNV, (2010), "Recommended Practice – Buckling strength of plated structures", DNV-RP-C201, Det Norske Veritas

APPENDIX A

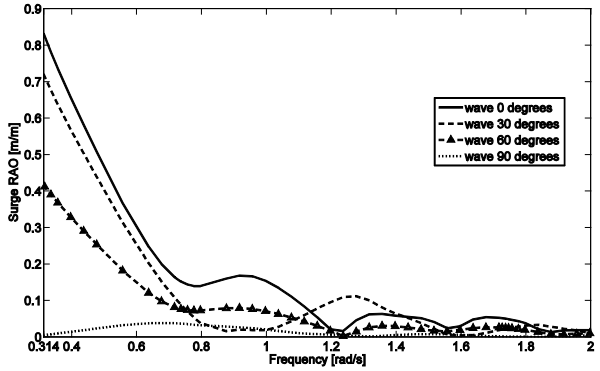

Figure 1. Surge RAO of the 5-MW-CSC

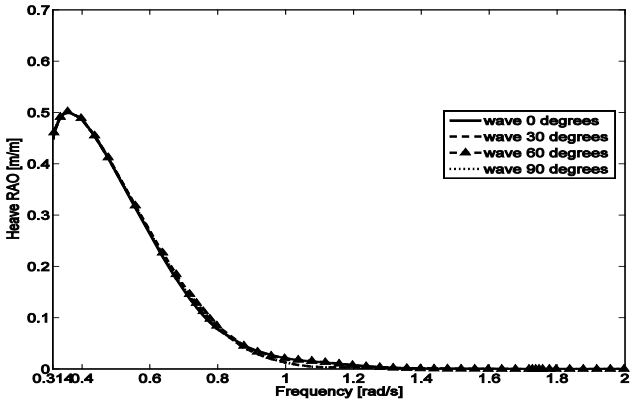

Figure 2. Heave RAO of the 5-MW-CSC

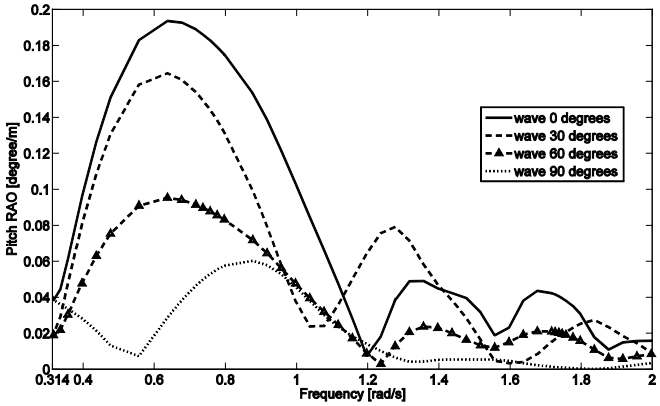

Figure 3. Pitch RAO of the 5-MW-CSC

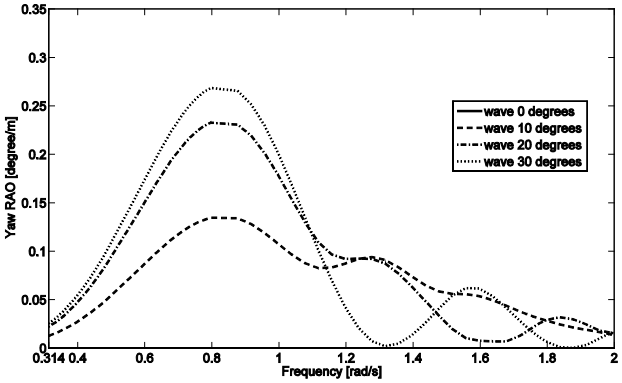

Figure 4. Yaw RAO of the 5-MW-CSC

APPENDIX B

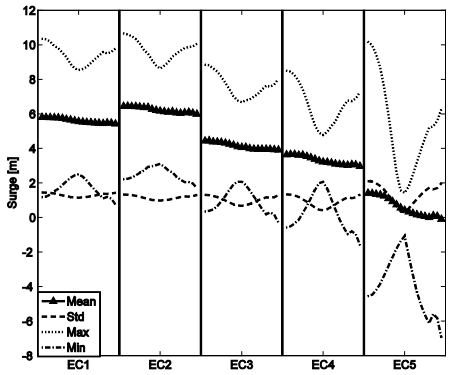

Figure 1. Statistical properties for surge motion of the 5-MW-CSC in extreme combined winds and waves. For each condition, from the left end to the right end, wave direction varies from 0 to 180 degrees with 10 degrees interval.

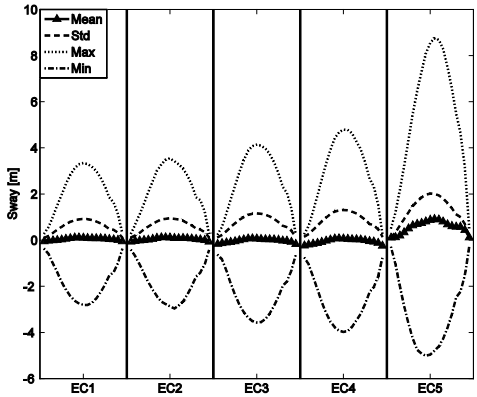

Figure 2. Statistical properties for sway motion of the 5-MW-CSC in extreme combined winds and waves. For each condition, from the left end to the right end, wave direction varies from 0 to 180 degrees with 10 degrees interval.

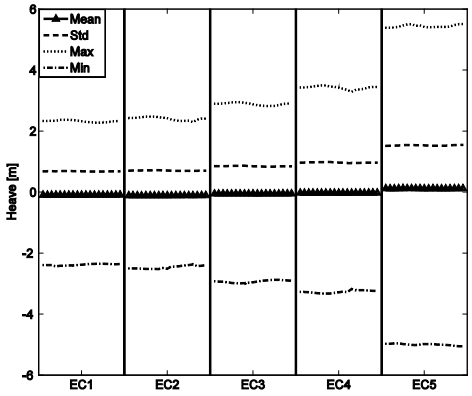

Figure 3. Statistical properties for heave motion of the 5-MW-CSC in extreme combined winds and waves. For each condition, from the left end to the right end, wave direction varies from 0 to 180 degrees with 10 degrees interval.

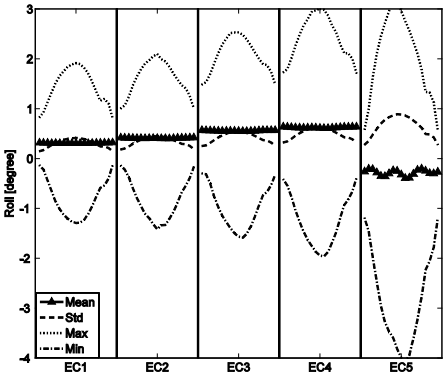

Figure 4. Statistical properties for roll motion of the 5-MW-CSC in extreme combined winds and waves. For each condition, from the left end to the right end, wave direction varies from 0 to 180 degrees with 10 degrees interval.

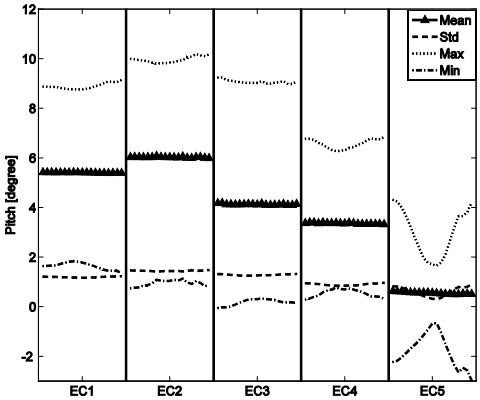

Figure 5. Statistical properties for pitch motion of the 5-MW-CSC in extreme combined winds and waves. For each condition, from the left end to the right end, wave direction varies from 0 to 180 degrees with 10 degrees interval.

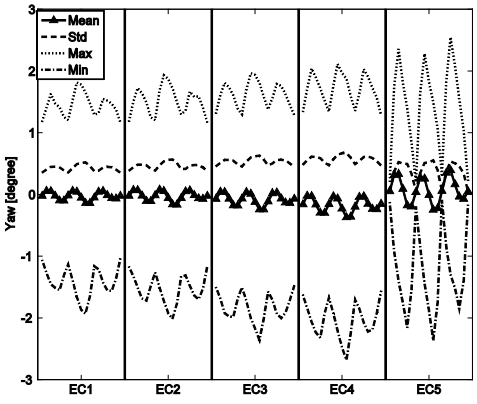

Figure 6. Statistical properties for yaw motion of the 5-MW-CSC in extreme combined winds and waves. For each condition, from the left end to the right end, wave direction varies from 0 to 180 degrees with 10 degrees interval.